Solar Energy 258 (2023) 28–36

Contents lists available at ScienceDirect

Solar Energy

journal homepage: www.elsevier.com/locate/solener

The impact of outdoor aging and soiling on the optic features of glass beads retro-reflective coatings

Alessia Di Giuseppe [a], Marta Cardinali [a], Beatrice Castellani [a,b,*], Mirko Filipponi [a,b], Andrea Nicolini [a,b], Federico Rossi [a,b]

[a] CIRIAF, Interuniversity Research Centre, University of Perugia, Via G. Duranti 63, 06125 Perugia, Italy
[b] Department of Engineering, University of Perugia, Via G. Duranti 67, 06125 Perugia, Italy

ARTICLE INFO

Keywords:
Urban Heat Island mitigation
Retro-reflective materials
Outdoor aging
Soiling
Spectrophotometric analysis
Angular reflection distribution

ABSTRACT

The latest research suggests the use of retro-reflective (RR) materials as innovative coating solutions for building envelopes and urban surfaces. This study aims at investigating the performance of RR materials after outdoor aging and soiling during summer 2021 in Perugia, Italy. Different glass beads RR coatings were realized with three substrate typologies, characterized by various roughness, and they were investigated in terms of their optic performance. Also diffusive (DIFF) coatings were made for comparison purposes. Variations in terms of solar reflectance and relative angular reflection distribution were compared with the same coatings in pre-aging conditions. Pre-aging optic data were presented and discussed in a previous work by the Authors. In all cases, the aged samples exhibit lower global reflectance values compared to their original conditions: the RR coating over a smooth pine wood substrate shows the highest reduction value equal to 14.4%. A stronger relative RR component was found for all the RR samples in post-aging conditions. Future developments may involve the identification of an optimal protective layer to be applied on RR materials to prevent the detachment of glass beads in RR post-aging coatings.

1. Introduction

Urban population is growing significantly, resulting in increased anthropogenic modification of natural landscape that determines a change of thermal and energy balance of cities. In fact, urban temperatures are higher than in nearby rural areas as a consequence of the fact that artificial surfaces typically absorb and store the solar radiation more than natural ones, increasing the Urban Heat Island (UHI) phenomenon [1]. The ongoing climate change contributes to the further worsening of UHI with negative influences as well as: increase of heat and pollution, reduction of thermal comfort, increase of building energy consumption and of peak electricity demand in summer [2–5].

In the last years, many research activities have been focused on the study and development of efficient mitigation strategies to counteract the urban overheating caused by UHI [6,7]. Innovative solutions such as high reflective, diffusive materials (i.e. cool roofs and cool pavements) [8–10] have been largely investigated as well as measures that improve earth surface reflectivity and proposed for building application. In fact, they have proven to be capable of maintain substantially lower superficial temperature as compared to conventional surfaces due to their intrinsic high albedo.

In addition to the traditional diffusive (DIFF) materials, retro-reflective (RR) materials have been investigated by the researchers during the last years thanks to their capability to reflect the sunlight predominantly towards the same direction of incidence [11]. In fact, RR materials have been presented as an effective solution to reduce building energy consumption for summer cooling and, moreover, to improve urban climate conditions during summer. Furthermore, RR materials could be effective also in bifacial photovoltaic fields, in increasing the energy reflected towards the downward photovoltaic panel, thus producing an enhancement of the produced electric energy. All the aforementioned strategies are also called high albedo solutions (HAS) and they allow to increase the terrestrial albedo, thus tackling global warming [12–14]. In fact, HAS effects involve at the same time: (i) the reduction of building energy consumption, especially in cooling dominant zones (CDZs), (ii) mitigation of the UHI phenomenon, and (iii) offset the CO_2 emissions.

Concerning RR materials, several studies have proved their cooling

* Corresponding author at: CIRIAF, Interuniversity Research Centre, University of Perugia, Via G. Duranti 63, 06125 Perugia, Italy.
E-mail address: beatrice.castellani@unipg.it (B. Castellani).

https://doi.org/10.1016/j.solener.2023.04.056
Received 27 May 2022; Received in revised form 10 November 2022; Accepted 24 April 2023
Available online 4 May 2023

effect, especially in Urban Canyons, since they could avoid the multiple reflections over building surfaces [15–17]. In Morini et al. (2018) [18], RR materials applied on vertical walls increase up to 5% the energy radiation reflected beyond an urban canyon [18].

However, the beneficial effects of RR materials can be affected by aging processes and soiling that modify their features and performance. In fact, weathering (i.e. UV radiation, temperature, and moisture), and soiling exposure (i.e. microbiological growth and deposition of the atmospheric aerosols) are the main causes of the material degradation over time.

Natural and artificial aging procedures have been tested and presented in literature in order to assess the long-term performance of RR materials. In Paolini et al. (2014) [19], a natural aging exposure of roofing membranes was performed in Italy. Results showed an average reflectance reduction of 0.18 after two years of natural exposure. In Morini et al. (2018) [20], laboratory accelerated aging tests, according to ASTM G154 were performed to evaluate the long-term performance of some RR tiles and paints for building application. Results showed that RR features were kept after the accelerated aging processes, since minimal changes in global reflectance and directional reflectivity occurred for the investigated RR aged samples with respect to the same specimens in pristine conditions [20]. In Yuan et al. (2018) [21], a long-term aging exposure of 368 days was performed for different glass beads RR samples, showing that no significant variations occurred in solar reflectance and angular reflection distribution after outdoor aging [21].

In this framework, the present paper aims to investigate the effect of natural aging and soiling exposure on the optic features of RR and DIFF coating samples made by different substrate materials. The same samples in pristine condition were already characterized in terms of their optic performance in a previous work by the Authors [22]. In this study, the optic performance of the aged samples was determined through a spectrophotometric and a directional reflection analysis. Then, the optic properties of the aged and pristine samples were analysed and compared in this study.

2. Materials and methods

In this section, the investigated samples were firstly described with a particular focus on their optic characteristics in pristine condition. Then, the applied methodology for the investigation of samples' optic performances after outdoor summer aging and soiling was described.

2.1. Description of samples

Three different substrate samples, i.e. smooth pine wood panel (SW), rough plywood panel (RW), and smooth acetate sheet (SA), were used in a previous work [22] in order to analyse the effect of the substrate on the RR coating's optic features. The RR coating samples were made by doping a high reflective white paint with RR glass beads evenly distributed on the material's top surface. RR glass beads with an average diameter of 0.1 ÷ 0.2 mm were tested. The RR coating samples are mentioned as RR_{SW}, RR_{RW}, and RR_{SA} made by SW panel, RW panel, and SA sheet respectively. DIFF samples coated only with the high reflective white paint were used as a reference case and are defined as $DIFF_{SW}$, $DIFF_{RW}$, and $DIFF_{SA}$. Both RR and DIFF samples in pristine condition were already characterized in terms of their optic performance in a previous work by the Authors [22]. Results showed that all DIFF samples performed higher global reflectance values compared to RR samples; in particular, among the diffusive samples, $DIFF_{SA}$ showed the highest value, equal to 83.6%, and among the RR samples, RR_{SW} exhibited the maximum global reflectance value equal to 74.8% [22]. Concerning the angular reflectivity characterization, RR_{RW} made by a rough substrate material, performed the highest relative retro-reflective component for high incident angles (i.e., from 0° to −50°), whilst the RR_{SA} made by a smooth substrate material, showed the highest relative percentage of retro-reflection for low angles of incidence (i.e., −60° and −70°) [22].

Fig. 1. DIFF and RR samples during the outdoor aging exposure.

RR_{RW} sample performed the highest relative retro-reflective percentage equal to 16.2% at 0° angle of incidence [22].

2.2. Methodology

Aging of DIFF and RR samples, involving outdoor weathering and soiling, was carried out during summer 2021 in Perugia, Italy. After the aging process, all RR and DIFF samples were characterized in terms of optic performances by a spectrophotometric analysis and an angular reflectivity investigation. Results were analysed and then compared with data of the same samples in pristine conditions.

2.3. Aging processes

The samples have been exposed to the most aging climate drivers for materials from 25th of June 2021 to 5th of October 2021 on the rooftop of the CIRIAF building, University of Perugia (43° 7′ 9.449'' N, 12° 21′ 27.451'' E): solar radiation, i.e. ultraviolet (UV) radiation, air temperature (T), relative humidity (RH), and rain precipitation. In Fig. 1 below, the samples during the outdoor aging exposure were shown.

In Figs. 2-4, T (°C), RH (%), global radiation (W/m^2) and rain precipitation (mm) during the aforementioned period were presented, as they affect the aging processes of materials in a predominant way (data source: fixed weather station settled above the rooftop level at the CIRIAF building, near the outdoor aging location). The daily mean value was calculated for the aforementioned parameters during the aging processes. Thus, according to the Fig. 2, the average T (°C) of the monitored period was equal to 23.2 °C with a maximum average T (°C) of 29.9 °C and a minimum average T (°C) equal to 16.9 °C. Concerning the RH parameter (Fig. 2), the monitored values obviously showed a very wide fluctuation with an average RH value equal to 51.5%. The average global reflectance value (Fig. 3) resulted equal to 267.6 W/m^2 during the considered period. Finally, rain precipitation was absent or not relevant in the considered period, as shown in Fig. 4.

2.4. Spectrophotometric analysis

Firstly, a spectrophotometric analysis was performed by a Shimadzu SolidSpec 3700 spectrophotometer equipped with 60 mm integrating sphere. The wavelength range of measurement is from 300 to 2500 nm, with a data interval of 5 nm. Datasheet of the spectrophotometer

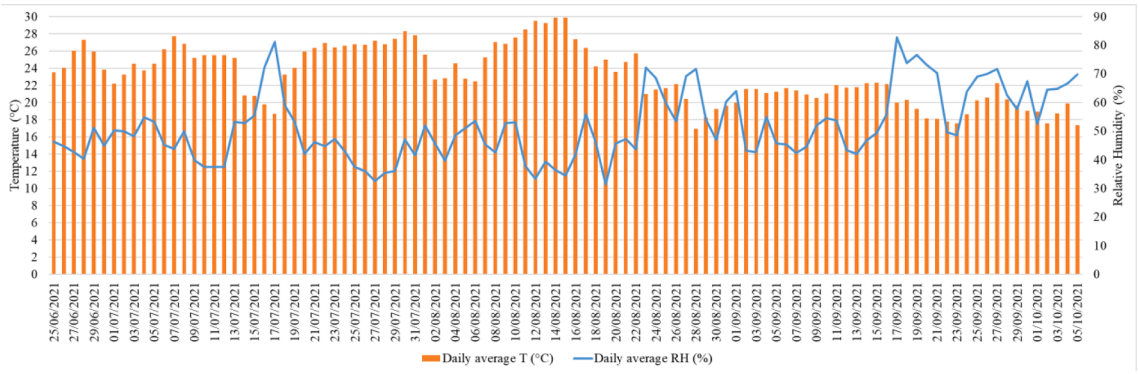

Fig. 2. Daily average T (°C) and RH (%) during the aging and soiling processes.

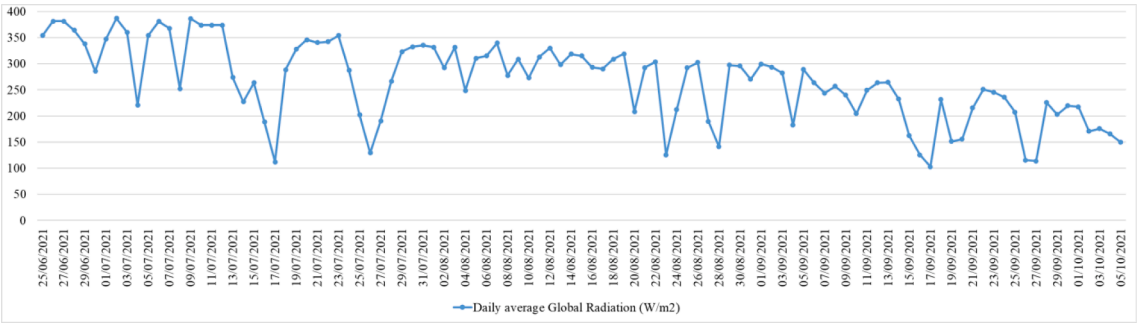

Fig. 3. Daily average Global Radiation (W/m^2) during the aging and soiling processes.

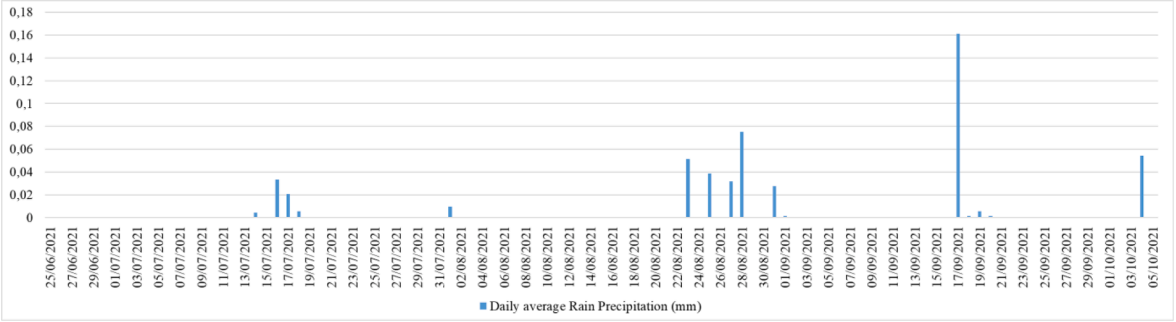

Fig. 4. Daily average Rain Precipitation (mm) during the aging and soiling processes.

equipment can be found in [24]. A total of three spectral reflectance measures have been carried out for each sample, allowing to obtain the average over the three measurements. Global reflectance of each sample was calculated according to ASTM Standard E 903–20 and ASTM Standard G 173–03. The aim is to investigate the reflectivity of the post-aging samples in terms of global hemispherical solar reflectance and its spectral distribution.

2.5. Angular reflectivity analysis

Finally, a directional reflectivity analysis was carried out in order to characterize the angular distribution of reflected radiation by each sample for different directions of incident radiation. The measurements were performed by an ad-hoc experimental facility, already introduced by the Authors in previous works [22,25], since the common testing equipment in-lab or in situ cannot be used to investigate the angular reflectivity properties of the samples. The experimental facility is composed by a semi-circular structure graduated every 10° and a LED light source. Irradiance measurements in W/m^2 have been performed in each angular position along the semi-circular structure through a photo-radiometer Delta-OHM HD 9221 with an LP9221/RAD probe [26]. In correspondence of the light source, two irradiance measures were carried out on both sides of the lamp. Then, the average value was calculated and considered for this angular position.

3. Results and discussion

In this paragraph results of the investigation of the samples' optic performances are presented and discussed.

3.1. Spectrophotometric characterization

Three spectrophotometric measurements were performed for each sample in order to over-come their superficial non-homogeneity, especially for the two wood-based samples. A comparison of the averaged reflectance measurements of pre- and post-aging samples over the wavelength range is shown in Figs. 5-7.

Both RR and diffusive post-aging samples show an overall lower

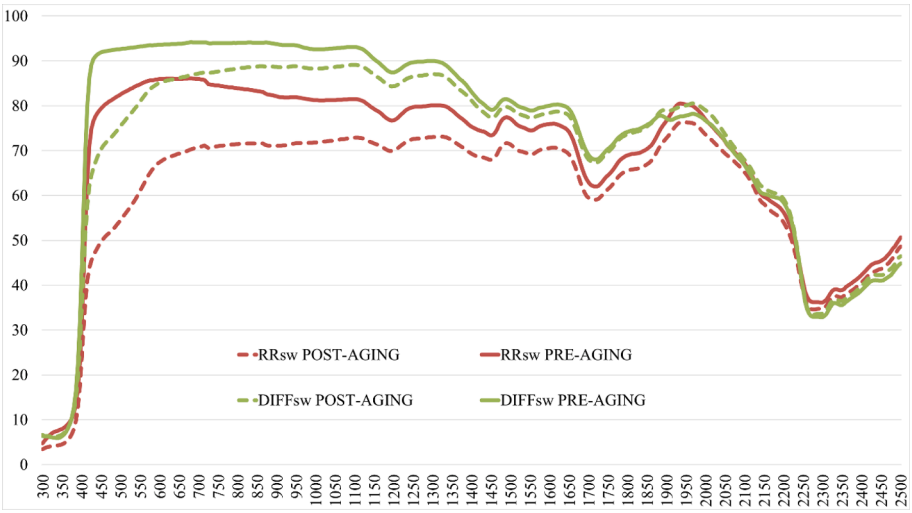

Fig. 5. Spectral reflectance of RR_{SW} and $DIFF_{SW}$ samples pre- and post-aging from 300 to 2500 nm.

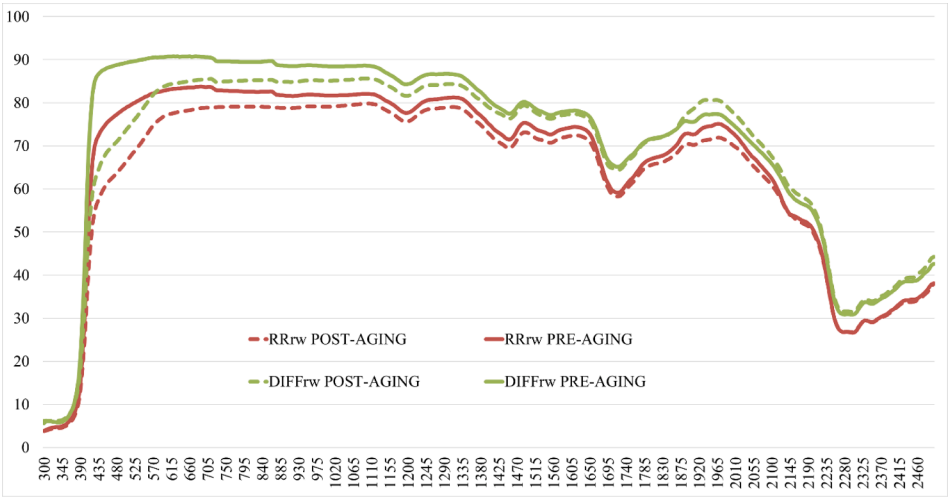

Fig. 6. Spectral reflectance of RR_{RW} and $DIFF_{RW}$ samples pre- and post-aging from 300 to 2500 nm.

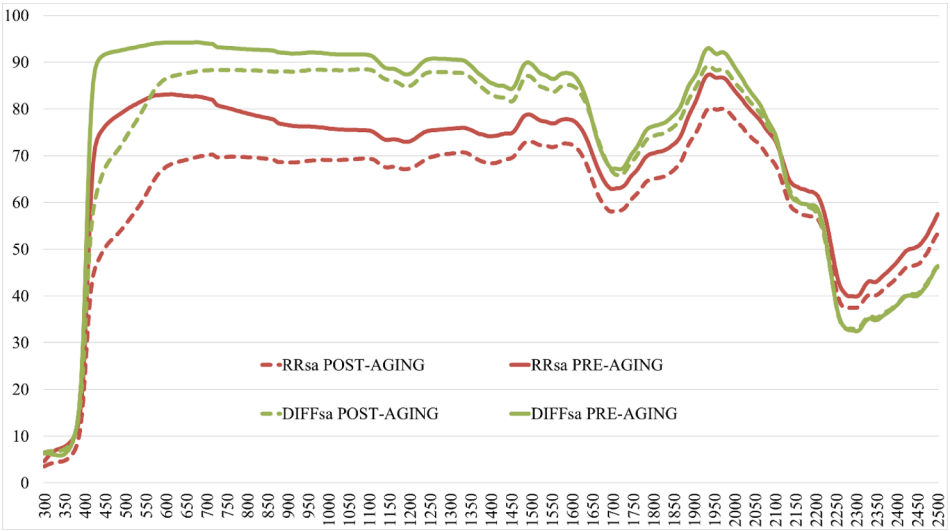

Fig. 7. Spectral reflectance of RR_{SA} and $DIFF_{SA}$ samples pre- and post-aging from 300 to 2500 nm.

Table 1
Global reflectance of samples before and after aging processes. *Results from a previous work of the Authors [22].

Samples	Global reflectance (%) PRE-AGING*	Global reflectance (%) POST-AGING	Δ (%)
RR_{SW}	74.8	60.4	−14.4
RR_{RW}	72.8	67.4	−5.4
RR_{SA}	71.7	59.7	−12
$DIFF_{SW}$	83.5	75.7	−7.8
$DIFF_{RW}$	80.1	73.5	−6.6
$DIFF_{SA}$	83.6	75.8	−7.8

reflectance, with minor exceptions; in particular:

- RR_{SW} sample: over 2000 nm, the reflectances of pre- and post-aging samples are very close to each other (see Fig. 5);
- $DIFF_{SW}$ sample: over 1705 nm, the reflectances of pre- and post-aging samples correspond almost exactly; in particular, the reflectance of post-aging sample goes beyond its corresponding pre-aging sample over 1870 nm (see Fig. 5);
- RR_{RW} sample: the reflectances of pre- and post-aging samples become very close to each other from 1700 to 1740 nm and from 2115 to 2500 nm (see Fig. 6);
- $DIFF_{RW}$ sample: over 1475 nm, the reflectance of post-aging sample corresponds almost exactly to pre-aging sample's reflectance; from 1855 to 2500 nm, the reflectance of post-aging sample goes beyond its corresponding pre-aging diffusive sample (see Fig. 6);

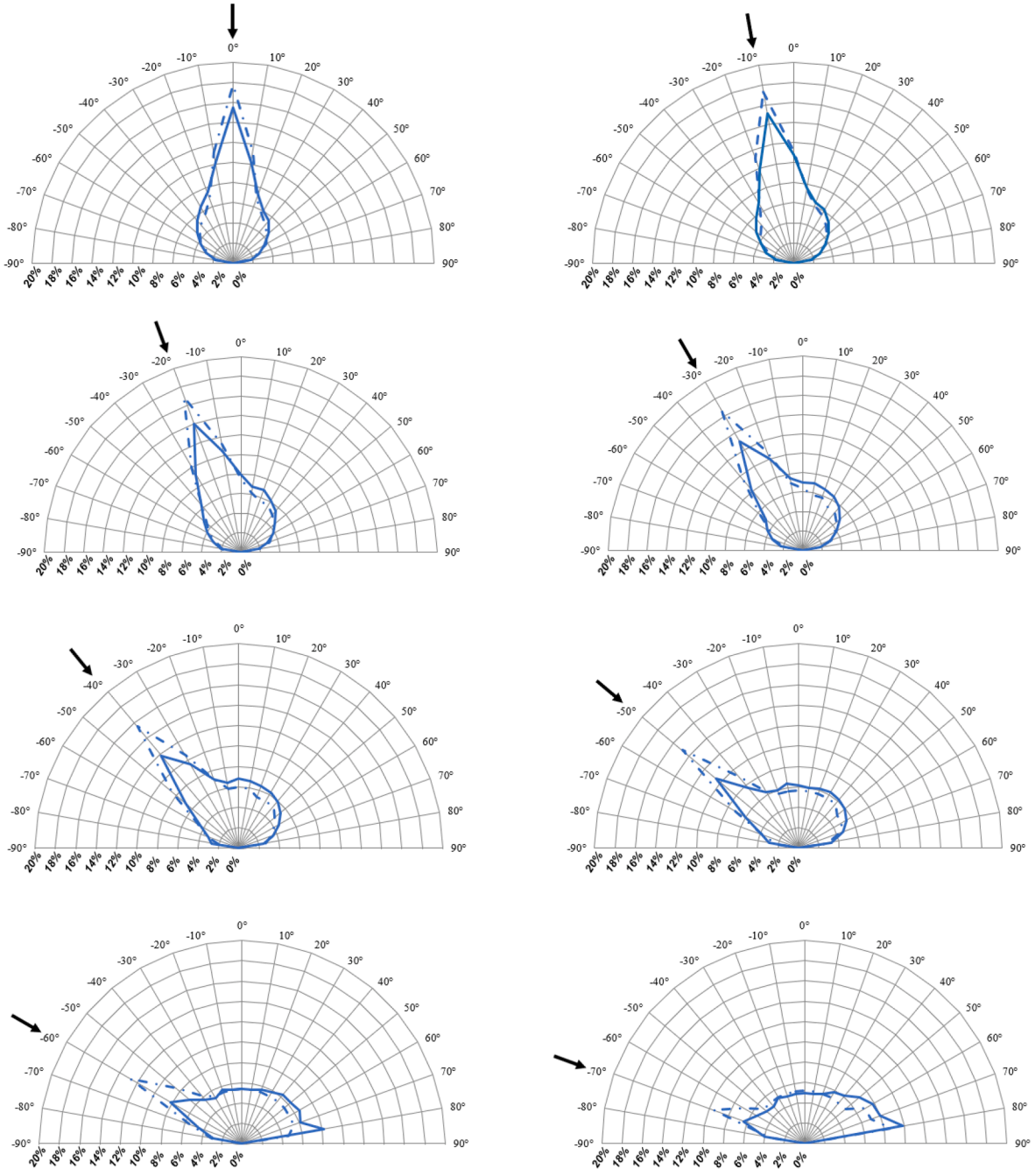

Fig. 8. Angular reflectivity profiles of RR_{SW} samples pre- and post-aging for each direction of incident radiation from 0° to −70°.

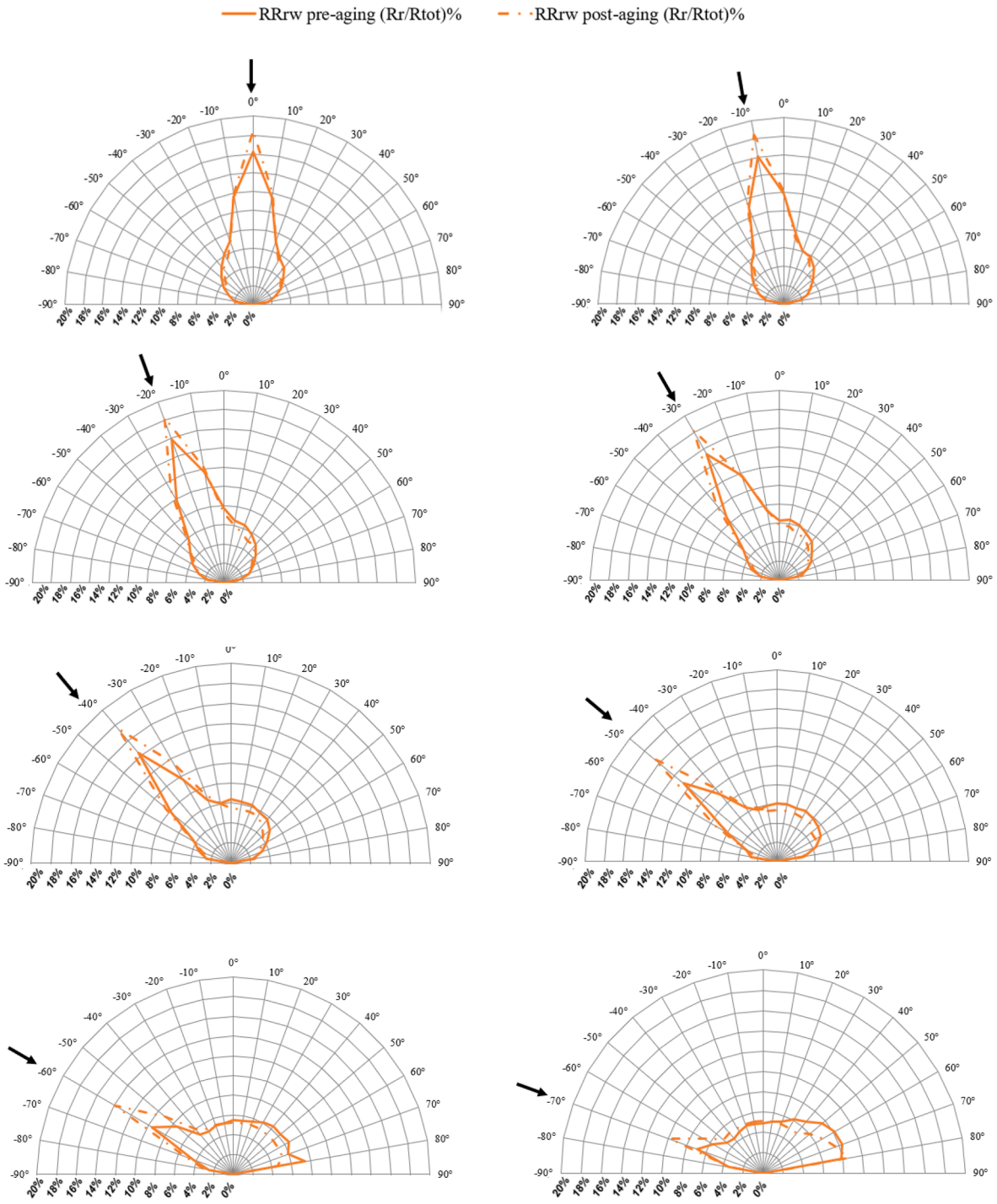

Fig. 9. Angular reflectivity profiles of RR_{RW} samples pre- and post-aging for each direction of incident radiation from 0° to −70°.

- RR_{SA} sample: from 2200 to 2255 nm, the reflectances of pre- and post-aging samples become very close to each other (see Fig. 7);
- $DIFF_{SA}$ sample: the reflectance of post-aging sample corresponds almost exactly to pre-aging sample's reflectance from 1640 to 1700 nm and over 2100 mn; in particular, from 1650 to 1680 nm, from 2115 to 2160 nm and over 2275 nm, the reflectance of post-aging sample goes beyond its corresponding pre-aging diffusive sample (see Fig. 7).

Global reflectance values are shown in Table 1. In all cases, the post-aging samples exhibit lower global reflectance values: the RR_{SW} sample's show the highest reduction value equal to 14.4% while all diffusive samples exhibit a reduction from 7% to 8%, as shown in Table 1. The Δ values (%) are calculated as the difference between the post-aging's global reflectance value and the pre-aging's one.

The post-aging sample's outcomes are consistent with the pre-aging sample's results [22]. In particular, all diffusive samples post-aging show a higher global reflectance with comparing to RR samples after the aging exposure: in fact, even if $DIFF_{SA}$ and $DIFF_{SW}$ samples exhibit the highest Δ values (-7.8%) with respect to the same samples in pristine condition, among the diffusive post-aging samples, they also confirm after the outdoor aging and soiling the highest global value equal to 75.8% and 75.7%, respectively. $DIFF_{RW}$ post-aging sample exhibits the lowest global reflectance value (73.5%), even if it shows the lowest Δ

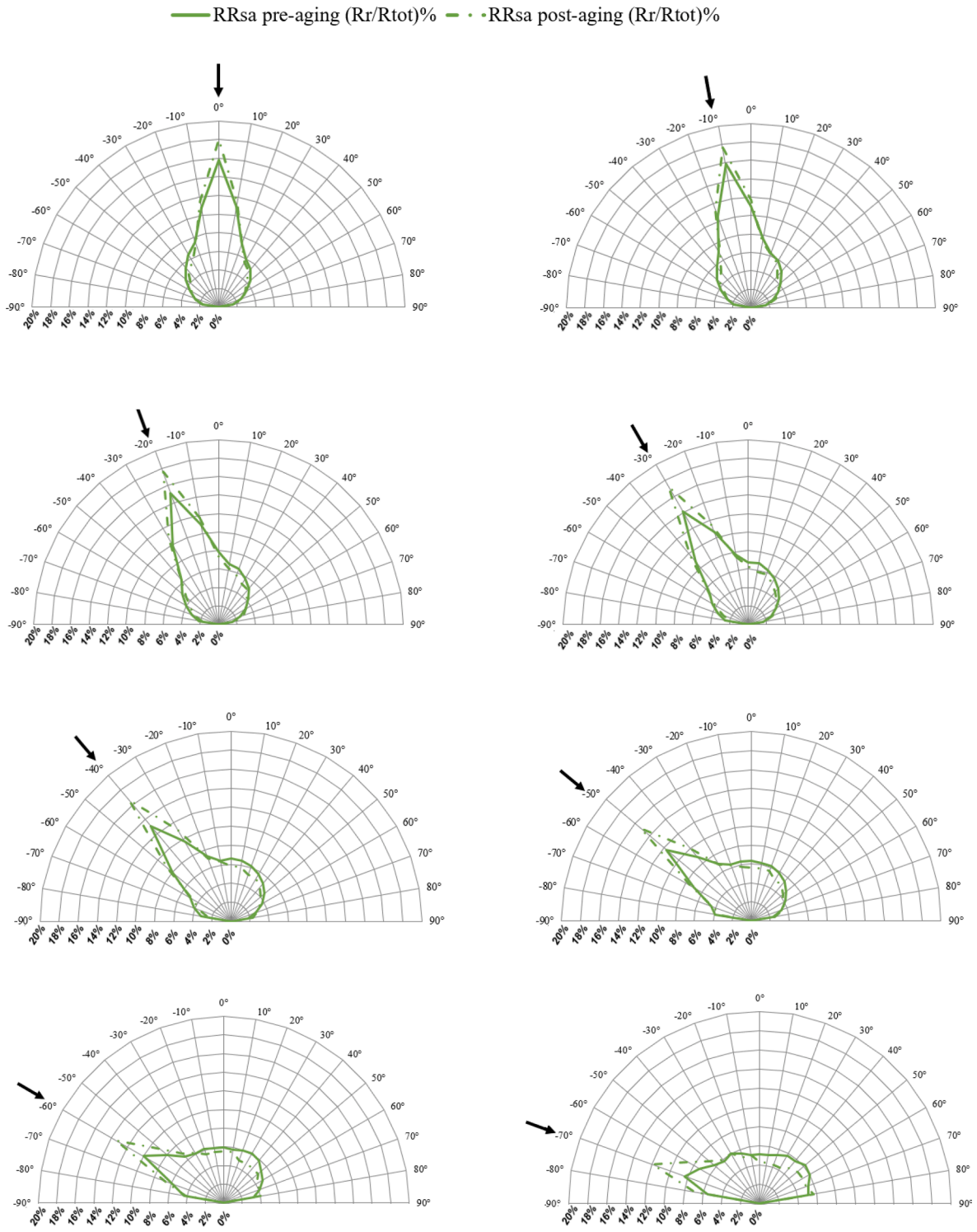

Fig. 10. Angular reflectivity profiles of RR_{SA} samples pre- and post-aging for each direction of incident radiation from 0° to −70°.

value (-6.6%) among the three diffusive samples post-aging. Consequently, among the diffusive post-aging samples, the aging exposure seems to affect more the samples characterized by a smooth substrate, both of pine wood and acetate sheet (i.e. $DIFF_{SW}$ and $DIFF_{SA}$) with respect to the $DIFF_{RW}$ sample made by a rough plywood substrate.

Considering the RR post-aging samples, RR_{SW} and RR_{SA} samples perform the highest Δ values equal to −14.4% and −12% respectively. Therefore, the aging process negatively affects the RR samples made by a smooth substrate (i.e. RR_{SW} and RR_{SA}), while it positively affects RR_{RW} characterized by a rough substrate which exhibits the lowest Δ value equal to −5.4% and also the highest global reflectance value (67.4%), among the RR post-aging samples. Thus, the roughest RR coating may prevent the detachment of glass beads as the surface is not homogeneous.

3.2. *Angular reflectivity characterization*

Concerning the angular reflectivity analysis, a stronger relative RR

Table 2
Relative retro-reflective component of each sample, before and after aging processes (i.e. the percentage of reflected radiation in the direction of incidence, over the sum of the reflection, for each sample). *Results from a previous work of the Authors [22]. .

Angle of incidence	Pre-aging*	Post-aging
	RR_{SW}	RR_{SW}
0°	15.5%	17.8%
−10°	15.1%	17.3%
−20°	14.0%	16.9%
−30°	13.0%	16.6%
−40°	11.8%	15.5%
−50°	10.5%	14.9%
−60°	8.2%	12.7%
−70°	6.3%	9.6%
	RR_{RW}	RR_{RW}
0°	16.2%	18.5%
−10°	16.1%	18.5%
−20°	15.8%	18.2%
−30°	15.4%	18.2%
−40°	14.3%	17.6%
−50°	12.7%	16.7%
−60°	9.6%	14.0%
−70°	6.9%	9.8%
	RR_{SA}	RR_{SA}
0°	15.9%	18.0%
−10°	15.8%	17.6%
−20°	15.1%	17.6%
−30°	14.2%	17.2%
−40°	13.0%	16.6%
−50°	11.7%	15.2%
−60°	10.0%	13.4%
−70°	8.4%	11.9%

component was found for all RR post-aging samples with comparing to the same pre-aging samples, for all incident of angles. A comparison of angular reflectivity distribution (i.e. from 0° to −70° angles of incidence) of RR_{SW}, RR_{RW}, and RR_{SA} samples, before and after aging processes, is shown in Figs. 8-10 below. The direction from which the incident radiation hit the tested sample is represented by the black arrow. The results are represented as the percentage ratio between the reflected radiation in a specific direction (W/m^2) over the total reflected radiation (W/m^2) in all directions, for each sample. Therefore, reflection percentages could be quantitatively compared only for the same sample's reflection distribution, and not between different samples.

A diffusive component is visible in all RR pre- and post-aging sample, but it is stronger in the RR pre-aging ones. In fact, it is clear that the diffusive component decreases in the RR post-aging samples due to the aging and soiling processes, resulting in a better relative RR post-aging performance. Also a smaller specular component occurs in all RR post-aging samples with respect to the pre-aging ones, for low incidence angle (i.e. from −50° to −70°).

All diffusive pre- and post-aging samples have a directional reflection distribution which follows the cosine's Lambert law for incident beams near to the direction normal to the sample, while for high incident angles a specular reflection occurs for all diffusive samples.

Values of the relative percentage ratio between the reflected radiation in the same direction of incidence and the total reflected radiation are reported in Table 2 for the pre- and post-aging RR samples.

The post-aging sample's outcomes are consistent with the pre-aging sample's results [22]: RR_{RW} sample is confirmed as the best performing both in pre-aging and in post-aging, among the RR tested samples; in fact, RR_{RW} post-aging sample presents the highest relative percentage of retro-reflection for high incident angles (i.e. from 0° to −60°). RR_{SA} post-aging sample performs slightly higher relative percentage values at −70° angles of incidence, with respect to the RR_{RW} sample. RR_{SW} post-aging sample exhibits the lowest relative percentage of retro-reflection for all incident angles.

4. Conclusions and further developments

The present work aims at investigating the performance of diffusive and RR substrate materials, characterized by a different roughness, after natural aging and soiling exposure. A smooth pine wood panel (SW), a rough plywood panel (RW), and a smooth acetate sheet (SA) were used as substrate materials to realize three RR (i.e., RR_{SW}, RR_{RW}, RR_{SA}) and three diffusive (i.e., $DIFF_{SW}$, $DIFF_{RW}$, $DIFF_{SA}$) coatings. All diffusive and RR samples post-aging were characterized in terms of optic performance through a spectrophotometer and an angular reflectivity analysis, using an ad-hoc experimental facility. In a previous work [22] the same samples in pristine conditions were characterized by the Authors. Results of the samples post-aging were analysed and compared with the pre-aging ones. The main findings are presented in the following points:

Concerning spectrophotometric analysis, all post-aging samples exhibit lower global reflectance values: the RR_{SW} sample's show the highest reduction value equal to 14.4% while all diffusive samples exhibit a reduction from 7% to 8%. The aging exposure seems to affect more the diffusive and RR samples characterized by a smooth substrate, both of pine wood and acetate sheet, with respect to the diffusive and RR samples made by a rough plywood substrate;

Concerning the angular reflectivity analysis, a stronger relative RR component was found for all RR post-aging samples with comparing to the same pre-aging samples, for all incident angles (from 0° to −70°). In fact, the diffusive relative component decreases in the RR post-aging samples due to the aging and soiling processes, resulting in a better relative RR post-aging performance;

The maximum relative retro-reflective capability is equal to 18.5% for sample RR_{RW} at 0° angle of incident radiation. RR_{RW} sample is confirmed as the best performing in terms of concentration of the reflected radiation around the incident direction, both in pre-aging and in post-aging, among the RR tested samples.

Further studies are foreseen with the aim of assessing an optimal protective layer to be applied on RR materials to prevent and/or reduce the detachment of glass beads in RR coatings. The influence of the protective layer on cooling effect of RR materials will be investigated in specific application, i.e. Urban Canyon configuration. In addition, the performance of RR materials covered by protective layer will be assess through natural outdoor aging and soiling.

Declaration of Competing Interest

The authors declare that they have no known competing financial interests or personal relationships that could have appeared to influence the work reported in this paper.

Acknowledgements

The present experimental research was funded by the Italian Ministry of University and Scientific Research (MIUR) under the PON Project entitled "BEST4U—Bifacial Efficient Solar Cell Technology with 4-Terminal Architecture for Utility Scale".

References

[1] Santamouris, M., 2015. Analyzing the heat island magnitude and characteristics in one hundred Asian and Australian cities and regions. Sci. Total Environ. 512–513, 582–598.
[2] Santamouris, M., Cartalis, C., Synnefa, A., Kolokotsa, D., 2015. On the impact of urban heat island and global warming on the power demand and electricity consumption of buildings −A review. Energy Build. 98, 119–124.
[3] Rossi, F., Anderini, E., Castellani, B., Nicolini, A., Morini, E., 2015. Integrated improvement of occupants' comfort in urban areas during outdoor events. Build. Environ. 93, 285–292.
[4] Rossi, F., Bonamente, E., Nicolini, A., Anderini, E., Cotana, F., 2016. A carbon footprint and energy consumption assessment methodology for UHI-affected lighting systems in built areas. Energy Build. 114, 96–103.

[5] Zinzi, M., Agnoli, S., Burattini, C., Mattoni, B., 2020. On the thermal response of buildings under the synergic effect of heat waves and urban heat island. Sol. Energy 211, 1270–1282.
[6] Akbari, H., Cartalis, C., Kolokotsa, D., Muscio, A., Pisello, A.L., Rossi, F., Santamouris, M., Synnefa, A., Wong, N.H., Zinzi, M., 2016. Local climate change and urban heat island mitigation techniques–the state of the art. J. Civ. Eng. Manag. 22, 1–16.
[7] Rossi, F., Pisello, A.L., Nicolini, A., Filipponi, M., Palombo, M., 2014. Analysis of retro-reflective surfaces for urban heat island mitigation: A new analytical model. Appl. Energy 114, 621–631.
[8] Synnefa, A., Dandou, A., Santamouris, M., Tombrou, M., Soulakellis, N., 2008. On the use of cool materials as a heat island mitigation strategy. J. Appl. Meteorol. Climatol. 47, 2846–2856.
[9] Cardinali, M., Pisello, A.L., Piselli, C., Pigliautile, I., Cotana, F., 2020. Microclimate mitigation for enhancing energy and environmental performance of Near Zero Energy Settlements in Italy. Sustain. Cities Soc. 53, 101964.
[10] Yuan, J., Emura, K., 2017. Farnham, C, Is urban albedo or urban green covering more effective for urban microclimate improvement?: A simulation for Osaka. Sustain. Cities Soc. 32, 78–86.
[11] Yuan, J., Emura, K., 2015. Farnham, C, A method to measure retro-reflectance and durability of retro-reflective materials for building outer walls. J. Build. Phys. 38, 500–516.
[12] Cotana, F., Rossi, F., Filipponi, M., Coccia, V., Pisello, A.L., Bonamente, E., Petrozzi, A., Cavalaglio, G., 2014. Albedo control as an effective strategy to tackle Global Warming: A case study. Appl. Energy 130, 641–647.
[13] Akbari, H., Menon, S., Rosenfeld, A., 2009. Global cooling: increasing world-wide urban albedos to offset CO2. Clim. Change 94, 275–286.
[14] Rossi, F., Cotana, F., Filipponi, M., Nicolini, A., Menon, S., Rosenfeld, A., 2013. Cool roofs as a strategy to tackle global warming: economical and technical opportunities. Adv. Build. Energy Res. 7 (2), 254–268.
[15] Yuan, J., Farnham, C., Emura, K., 2015. Development of a retro-reflective material as building coating and evaluation on albedo of urban canyons and building heat loads. Energy Build. 103, 107–117.
[16] Rossi, F., Castellani, B., Presciutti, A., Morini, E., Anderini, E., Filipponi, M., Nicolini, A., 2016. Experimental evaluation of urban heat island mitigation potential of retro-reflective pavement in urban canyons. Energy Build. 126, 340–352.
[17] Rossi, F., Morini, E., Castellani, B., Nicolini, A., Bonamente, E., Anderini, E., Cotana, F., 2015. Beneficial effects of retroreflective materials in urban canyons: Results from seasonal monitoring campaign. J. Phys. Conf. Ser. 655, 012012.
[18] Morini, E., Castellani, B., Anderini, E., Presciutti, A., Nicolini, A., Rossi, F., 2018. Optimized retro-reflective tiles for exterior building element. Sustain. Cities Soc. 37, 146–153.
[19] Paolini, R., Zinzi, M., Poli, T., Carnielo, E., Mainini, A.G., 2014. Effect of ageing on solar spectral reflectance of roofing membranes: natural exposure in Roma and Milano and the impact on the energy needs of commercial buildings. Energy Build. 84, 333–343.
[20] Morini, E., Castellani, B., Nicolini, A., Rossi, F., Berardi, U., 2018. Effects of ageing on retro-reflective materials for building applications. Energy Build. 179, 121–132.
[21] Yuan, J., Emura, K., Farnham, C., 2018. A study on the durability of a glass bead retro-reflective material applied to building facades. Prog. Org. Coat. 120, 36–48. https://doi.org/10.1016/j.porgcoat.2018.03.009.
[22] Di Giuseppe, A., Cardinali, M., Castellani, B., Filipponi, M., Gambelli, A.M., Postrioti, L., Nicolini, A., Rossi, F., 2021. The effect of the substrate on the optic performance of retro-reflective coatings: An in-lab investigation. Energies 14.
[24] Website of Spectrophotometer C101-E167 SolidSpec-3700i/3700i DUV Datasheet. Available online: Shimadzu.com (Accessed on 3 May 2022).
[25] Gambelli, A.M., Cardinali, M., Filipponi, M., Castellani, B., Nicolini, A., Rossi, F., 2019. A normalization procedure to compare retro-reflective and traditional diffusive materials in terms of UHI mitigation potential. Proc. AIP Conf. Proc. 2191, 020085.
[26] Datasheet of Delta OHM HD9221 photo-radiometer with an LP9221/RAD probe. Available online at https://docs.rs-online.com/0053/0900766b80115ee0.pdf (Accessed on 09 May 2022).